GEOCHEMISTRY AND STRATIGRAPHIC CLASSIFICATION OF SANDSTONES OBSERVED BY THE MSL CURIOSITY ROVER S. Y. Khan[1] and K. M. Stack[2], [1]Massachusetts Institute of Technology, 77 Massachusetts Avenue, Cambridge, MA 02139 (syked@mit.edu), [2]Jet Propulsion Laboratory, 4800 Oak Grove Drive, Pasadena, CA 91104 (kathryn.m.stack@jpl.nasa.gov)

Introduction: Trends in bulk geochemistry can be used to constrain the provenance and possible stratigraphic position of sedimentary rocks. During the past ~8 years on the surface in Gale Crater, the Mars Science Laboratory (MSL) Curiosity rover has encountered sandstones within the 3 main stratigraphic units it has explored: the Bradbury group, Murray formation of the Mount Sharp group, and Stimson formation. Intermittently throughout the ~24 km traverse, Curiosity has observed sandstone outcrops whose stratigraphic context is unclear, either as a result of outcrop location, unusual lithology and geochemistry, or a lack of contextual data (e.g. Fig. 1). This study utilizes the large collection of targets sampled by the ChemCam instrument to characterize the bulk geochemistry of sandstones within each unit, permitting the target chemistries of the "unclassified" sandstones to be directly compared to the full dataset. Through this analysis, we seek to define a method by which unclassified targets can be better placed within a known stratigraphic context.

Data and Methods: Abundances of SiO_2, Al_2O_3, MgO, FeOT, CaO, Na_2O and K_2O measured by the ChemCam instrument were analyzed for all sandstone targets from Bradbury landing to the Glen Torridon region (sol 0 - 2737). ChemCam points on soil, obvious diagenetic features such as veins, and float blocks that could not be traced to a local source were excluded from the analysis. Targets were categorized by visual assessment of the grain size using images from the ChemCam Remote Micro-Imager (RMI) (fine, medium and coarse sandstone) to minimize potential grain size effects on geochemistry [1], and were grouped as Bradbury, Murray, or Stimson according to the designations of [2] and [3]. Major element oxides for

Figure 2. ChemCam RMI mosaic of Amargosa Valley sandstone Anvil Spring Canyon merged with Mastcam M-100, located at the transition between the Bradbury group and the Murray formation (image credit: William Rapin).

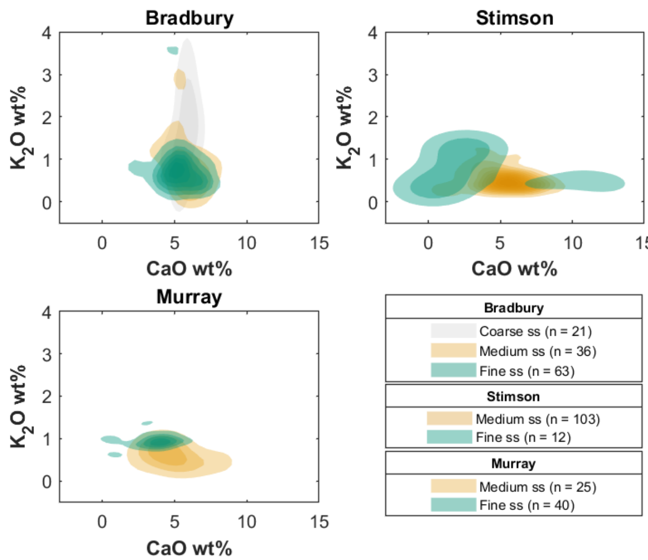

Figure 1: Grain size density contours for sandstones, averaged by target with bin size of 50. Contour levels are adjusted according to sample size. The population of coarse Stimson and Murray sandstones is not substantial enough to be included here.

each stratigraphic unit were plotted as density contours in order to visualize their distributions (Figs 2. and 3). The compositions of "unclassified" sandstones from Amargosa Valley (Anvil Spring Canyon, Copper Queen, Epaulet Peak, Upheaval Dome), Artists Drive (Little Devil), Logan's Run near Marias Pass (Albert, Charity, Tierra Blanca), and Ireson Hill (Quimby, Passagassawakeag, Wassataquoik) were overlaid on the density contours to qualitatively assess their fit to the three stratigraphic units.

Results: Density contour analysis by grain size indicates widely variable chemistries within the Stimson and Murray formations for fine- and medium-grained targets, with sizable variations occurring in Na_2O, FeOT and CaO space (Fig. 2) [4]. As most of the unclassified sandstones examined in this study were medium-grained sandstones, they are displayed and compared exclusively to the medium grained targets from the Bradbury, Murray and Stimson formations. Fig. 3a and 3b support the use of K_2O as a distinguishing feature of the Bradbury formation [5], although it is not systematic as shown by the substantial overlap with the Murray and Stimson targets. Though SiO_2 largely overlaps across all three units as well, Stimson sandstones feature particularly high SiO_2 contents (Fig.

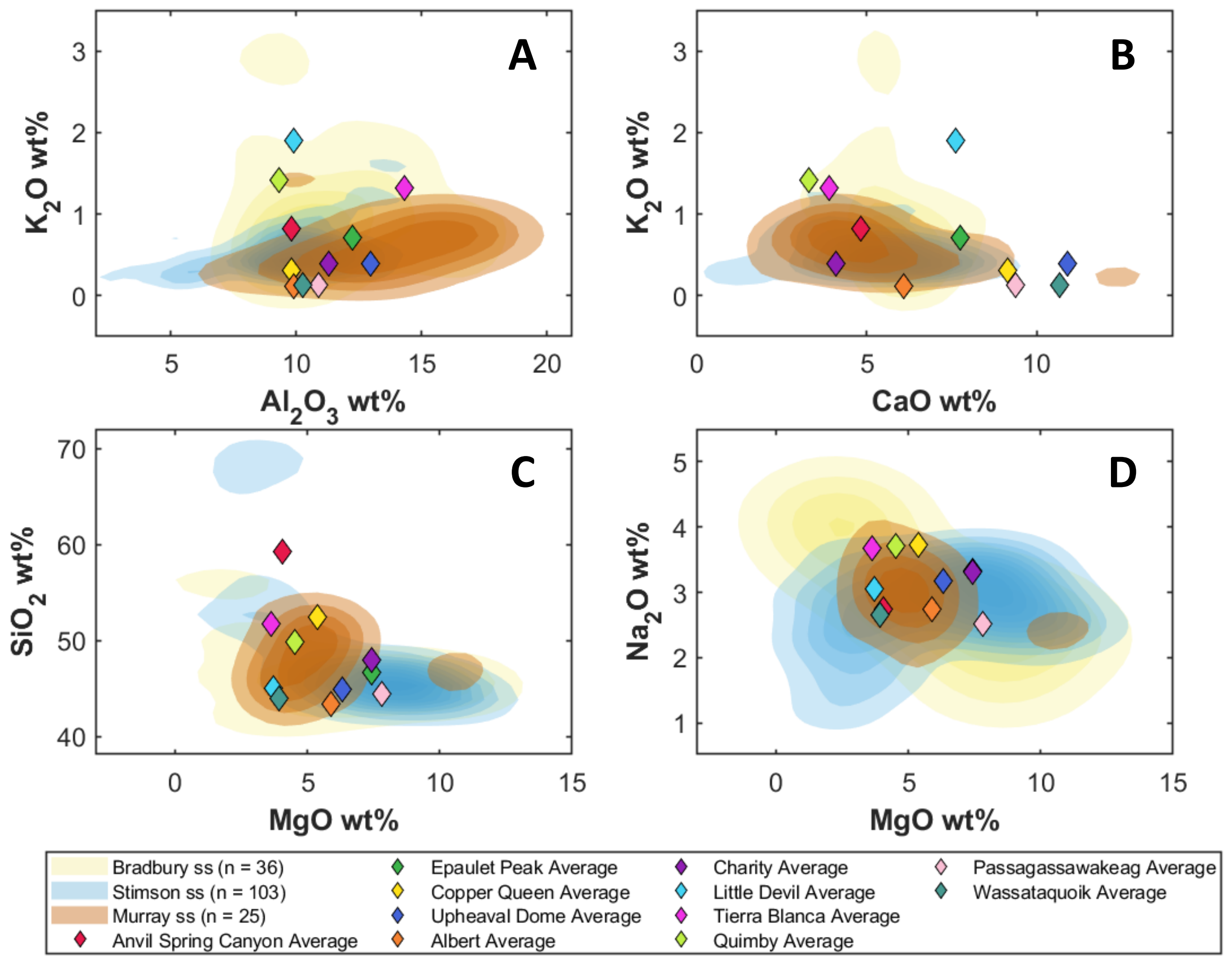

Figure 3: Density contours of medium-grained sandstones for select major element oxides, averaged by target and grouped by stratigraphic unit. Each density contour is a 2D histogram with a bin size of 50, which is smoothed using kernel density estimation. Contour lines connect points with the same probability density value and are adjusted according to the number of targets per unit (Bradbury lines = 5, Murray lines = 4, Stimson lines = 10). Stars denote average chemistry of unclassified sandstones.

3c) [6]. Murray sandstones are shown to have two prominent MgO peaks (Fig 3d) and comparable, though diminished, double peaks in CaO (Fig 3b) that are not reflected in the Bradbury and Stimson distributions.

A majority of the unclassified sandstones analyzed in this study fall in the overlap between Bradbury, Murray and Stimson compositions, which generally corresponds to the highest density contours, and thus cannot easily be classified as a particular stratigraphic unit based on their ChemCam compositions alone. However, several of the "unclassified" sandstones do appear to be a better fit to a particular unit. Anvil Spring Canyon's composition closely matches the secondary peak unique to Stimson in SiO_2. Little Devil and Quimby likewise trend with the high K_2O content of Bradbury formation sandstones. Though less pronounced, Copper Queen and Passagassawakeag display similarities to both the Stimson and Bradbury distributions.

Discussion: Substantial overlap in bulk geochemistry between the Bradbury, Murray, and Stimson sandstone populations is consistent with reworking of common source rocks into sedimentary units [7]. Consequently, unclassified sandstones that fall within this overlap are difficult to classify definitively based on ChemCam pairs of elements, leaving open questions regarding their stratigraphic context. Sandstones enriched in K_2O, SiO_2, Al_2O_3, MgO and CaO are most easily categorized using this method due to their clear association with stratigraphic trends observed for these oxides.

References: [1] Rivera-Hernandez et al. (2019) *Icarus 321*. [2] Grotzinger et al. (2015) *Science 350(6257)*. [3] Fedo et al. (2018) *LPSC,* Abstract #2083. [4] Bedford et al. (2020) *Icarus 341*. [5] Siebach K.L. et al. (2017) *JGR 122(2)* 295-328. [6] Frydenvang J. et al. (2017) *GRL 44(10)* 4716-4724. [7] Bedford et al. (2019) *GCA 246* 234-266.